

Pyrite Oxidation Rates from Laboratory Tests on Waste Rock

Kim Lapakko¹ and Edward Trujillo²

1. *Minnesota Department of Natural Resources, USA*
2. *University of Utah, USA*

ABSTRACT

Fourteen samples of pyrite-bearing waste rock were characterized (particle size distribution, chemistry, mineral content, degree of pyrite liberation, extent of precipitate coating on pyrite) and subjected to dissolution testing for 52 weeks. Approximately one-kilogram samples ($0.18 \leq d < 6.25$ mm) were placed into cells similar to that described in ASTM D5744-13. The modified testing procedure was divided into three phases. First, in the leach phase, the sample was soaked with 500 mL of deionized water for one hour, after which the leachate was collected in a flask for two hours then left exposed to ambient conditions for the rest of the day. Second, a drying phase started on the second day by pumping dry air (1 L/m) into the bottom of the cell for three days. Third, after drying, the humidity cell was kept unattended with the top lid on for the remaining three days. Leachate was analyzed for pH, sulfate, a number of other solutes, and bacterial growth. Pyrite was reported to be absent from four samples, at concentrations of 0.01 to 0.1 percent in three samples, and in the range of 0.7 to 4 percent in the remaining seven samples. Rates of pyrite oxidation were determined for all samples in which pyrite was detected, using sulfate release rates during weeks 37 to 52 and the calculated exposed pyrite surface area. For samples with pyrite contents of at least 0.7 percent, the oxidation rates determined were reasonably consistent with those predicted in the literature. For this same subset, oxidation rates for samples producing acidic drainage (~3.3-3.8) were one to twelve times those for samples producing circumneutral drainage (~7.0-7.5).

Keywords: pyrite oxidation rates, kinetics, humidity cell, laboratory weathering, mine rock drainage quality prediction

INTRODUCTION

Pyrite oxidation is a major concern related to waste rock excavated during mining operations. Pyrite and other iron-bearing sulfide minerals oxidize in the presence of oxygen and water and can produce acid, as well as iron oxyhydroxides and sulfate (reaction 1). Some or all of the acid produced can be neutralized by reaction with other minerals present in the rock. The acidity of drainage from an unmitigated waste rock facility is ultimately dependent on the balance of acid-producing and acid-neutralizing reactions. If the rate of acid production exceeds the rate of acid neutralization the drainage will be acidic. Quantification of pyrite oxidation rates and the attendant acid production benefits interpretation of kinetic test data, extrapolation of laboratory data to the field, and is required to model waste-rock drainage quality based on waste-rock composition.



Monomineralic dissolution studies have been conducted to determine rates of pyrite oxidation in oxygen saturated water (Williamson and Rimstidt, 1994) and in the presence of moist air (Jerz and Rimstidt, 2004). Using a method approximating that of Option B of ASTM D5744-13e (ASTM International 2013) for weathering a suite of greenstone rock samples, Lapakko and Antonson (2006) attributed sulfate release to oxidation of pyrite in the fine fraction in which water was retained. The pyrite oxidation rates determined were in good agreement with those presented by Williamson and Rimstidt (1994) for abiotic oxidation of pyrite by oxygen.

Jerz and Rimstidt (2004) conducted laboratory experiments at 25 °C, 96.7 % relative humidity, and oxygen partial pressures of 0.21, 0.61, and 1.00 atmosphere (atm). They derived the following expression for the rate of pyrite oxidation in moist air:

$$\frac{dFeS_2}{dt} = 10^{-6.6} P^{0.5} t^{-0.5} \quad (2)$$

where, $dFeS_2/dt$ is the rate of pyrite oxidation ($\text{mol m}^{-2} \text{s}^{-1}$), P is the partial pressure of oxygen (atm) and t is time in seconds. They reported that the reaction rate decreased over time due to formation of a precipitate layer on the mineral surface that inhibited oxygen transport.

The present humidity-cell studies were conducted using a one-day period for rinsing and draining of the cell followed by a three-day period during which dry air was introduced to the cell. After the drying cycle samples were retained undisturbed in the cells. The conditions for pyrite oxidation were consequently much dryer than those used by Lapakko and Antonson (2006), and may simulate conditions near the boundary of waste rock piles in an arid environment. The following

sections investigate pyrite oxidation rates for 10 waste-rock samples under these conditions and compare them to rates published for monomineralic pyrite oxidation studies.

METHODS

Materials

Fourteen rock samples for humidity-cell testing were collected from waste-rock piles (7 samples), outcrops (6 samples) and scars (1 sample) at the Questa molybdenum mine in northern New Mexico (Chevron, 2005). Samples from the waste-rock piles were collected from trenches (McLemore et al., 2005), homogenized and sieved to obtain the size fraction finer than 6.35 mm (McLemore et al., 2008). Rock samples were staged crushed with 1.27- and 0.635-cm jaw crushers to obtain the -0.635 cm size fraction (McLemore et al., 2008). Due to concerns regarding flow transmission during humidity-cell testing, all samples were dry-sieved to remove the fraction finer than 0.18 mm prior to testing. Dry sieving employing 12 Tyler screens was used to determine particle size distributions of the bulk sample, the sample submitted for humidity-cell testing, and the samples following termination of the humidity-cell tests.

The resultant samples were subjected to chemical, mineralogic, and petrographic analysis (McLemore et al., 2008; 2009). Mineral Services (2008) provided descriptions of hand samples, microscopic analysis of thin sections, Rietveld x-ray diffraction analyses, and analyses by scanning electron microscopy (SEM) with energy-dispersive x-ray spectrometry (EDS). Pyrite contents used in the present paper were selected based on consideration of chemical analyses and mineralogic analyses by both New Mexico Tech and Mineral Services. Pyrite grain-size distributions (McSwiggen, 2008a) and the extent of pyrite coating were also determined (McSwiggen, 2008b).

Humidity Cell Tests

Humidity-cell testing was performed at room temperature using a modified version of ASTM D5744-13e (ASTM International, 2013) for one year. Approximately one kilogram of sample was charged to each cell. The modified testing procedure was divided into three phases, i.e., (1) leach phase, (2) drying phase and (3) stand-alone phase over a seven-day cycle. During the first day (the leach phase), 500 mL of deionized water (or synthetic water) was delivered to the cell from the separatory funnel and the sample was allowed to soak for one hour. The leachate was then collected in a flask for two hours, after which the humidity cell was left undisturbed. Leachate was analyzed (1) directly for temperature, pH, and Eh; (2) after filtration (0.45 μ m) for sulfate, fluoride, and ferrous iron; and (3) after filtration and acidification (ultrapure nitric acid) for cations. The drying phase started on the second day by pumping air dried to a dew point of -40 °C (Balston model 76-10 membrane air dryer) at 1.0 liter/minute from the bottom of the cell for three days. After drying, the humidity cell was left alone for the remaining three days. Dry air flow rates, temperatures, pressure drops and humidity were measured for each cell periodically. Cell masses before and after the leach and after the dry-air portion of each weekly cycle were determined.

Samples used for the GHN-KMD-0088 cells were inoculated and analyzed for bacteria growth at weeks 5, 26, 38, 50, and 52. All leachate samples were analyzed in duplicate using MPN tests at 24 °C (Richins et al. 2008). The microbial humidity-cell inoculum was produced from rock samples from the mine that were provided for characterization and inoculum production. The inocula were produced using characterized media for enhanced growth of each general population group. The inocula were a unique composite of separately produced populations of (1) general heterotrophic species, (2) general sulfate-reducing species, (3) general *Acidithiobacillus* and *Leprotspirillum* species, (4) general acidophilic species, and (5) general *Archaea* species. The inocula contained concentrations of the five generalized population groups that mirrored the relative concentrations in the original sample.

Calculations

Pyrite grain size and liberation were determined in two steps (McSwiggen 2008a). First, the average pyrite grain size was determined for particles with diameters ranging from roughly 1 to 3 mm. The image analysis program NIH ImageJ was used to interpret backscatter electron signals collected using a JEOL 8600 Electron Probe Microanalyzer. The image analysis program identified sulfide mineral grains and determined the longest length, perimeter, and area of each grain. The “circular diameter” (diameter assuming a circular particle = $4 \times \text{particle area} / \text{particle perimeter}$) of each particle and total grain area present were calculated. The resultant data were sorted from smallest to largest particle area, and the percent cumulative areas for the sorted grains were calculated. The median grain diameter was defined as the circular diameter for which the percent cumulative area was 50. The probability of a sulfide grain being exposed was then calculated using the following equation:

$$P = 100 - 100[(R_1 - R_2)^2 / R_1^2] \tag{3}$$

- P = probability of sulfide grain being exposed,
- R₁ = radius of host rock grains,
- R₂ = median radius of all pyrite

Rates of pyrite oxidation were determined by dividing molar rates of sulfate release by twice the liberated pyrite surface area. Sulfate release rates were determined for periods from 6 to 9 and 37 to 52 weeks. The rate for a specific period was calculated by averaging the weekly sulfate release rates observed during the period.

The exposed pyrite surface area of a sample was determined by summing the exposed pyrite surface area in each particle size fraction, which was calculated as follows:

$$A_{py,i} = \left(\frac{\% FeS_2}{100} \right) \left(\frac{6}{\rho d_{gm,i}} \right) \left(\frac{M_i L_i (SR)}{100} \right) \quad (4)$$

where

- $A_{py,i}$ = pyrite area in particle size fraction i, m²,
- %FeS₂ = percent pyrite of sample, assumed to be constant among size fractions,
- ρ = pyrite density = 5.02×10^6 g m⁻³,
- $d_{gm,i}$ = geometric mean diameter of particle size fraction i, m,
- M_i = mass of rock in particle size fraction i, g,
- L_i = percent pyrite exposure in particle size fraction i, and
- SR = surface roughness factor for pyrite estimated as 4.9, the mean of five literature values presented by Lapakko and Antonson (2006).

RESULTS

Rock Characterization

The rocks examined were collected from rock piles and outcrops at the Questa mine site and reflected characteristics of the andesitic lava and rhyolitic ignimbrite rocks at the site (Dunbar, Heizler & Sweeney, 2008). Mineralogical analyses indicated that pyrite was absent from four of the samples and this paper will focus on the remaining ten samples. Six of these samples were from rock piles and four were collected from outcrops. Six of the samples were classified as andesite and four as rhyolite, with respective QSP alteration ranges of 0 to 90 percent and 0 to 70 percent (McLemore et al. 2008).

Particle size distributions for the humidity cell samples revealed that one to five percent of the sample mass was generally finer than 0.18 mm. Samples had been dry-sieved with the intent of removing this fraction but this method was not entirely effective. In particular sample BCS-VWL-0004 had about seven percent reporting as finer than 0.18 mm. Particle size distributions for five of the samples appeared to provide a central tendency for these data. The respective ranges for percent finer than 1.7 mm and 0.5 mm for these samples were 36 to 47 percent and 14 to 17 percent. Two samples were coarser and three finer than these samples.

Major whole rock components (and typical ranges) were SiO₂ (60-70 wt. %), Al₂O₃ (13-14 wt. %), total FeO and K₂O (both 3-5 wt. %). Respective sulfide and sulfate content ranges for the samples were 0.03-2.49 wt. % and 0.04 to 0.55 wt. % (Table 1). Although carbon contents of eight of the ten samples did not exceed 0.07 percent, one value was reported as 1.58 wt. % for a sample in which wood fragments were detected (BCS-VWL-0004; Table 1). Quartz was typically the dominant mineral present (19-51 wt. %), and other major minerals were potassium feldspar (5-27 wt. %), illite-sericite (9-33 wt. %), and plagioclase (<1 – 30 wt. %) (McLemore et al. 2008).

Pyrite was the dominant sulfide mineral present, with jarosite and gypsum observed in some samples (Table 1). New Mexico Tech estimated jarosite and gypsum contents based on the sulfate content determined by chemical analysis, but the presence of these minerals was verified by petrographic examinations in six and two samples, respectively. Similarly, calcite contents were estimated assuming all carbon was present as calcite but its presence was verified in only three samples (Table 2).

Pyrite contents ranged from 0.01 to 4 wt. % (Table 1). Based on examination of 89 to 1033 pyrite grains per sample, median pyrite diameters ranged from 12 to 1100 μm (Table 1). It should be noted that the median values were selected as the 50th percentile of cumulative area, and they do not reflect the large number of very fine pyrite grains in the samples. The percentage of pyrite particles finer than 10 μm ranged from roughly 60 to 90 percent. However, with one exception, the fraction of the total pyrite surface area contributed by this fine fraction did not exceed 7.2 percent. Based on the particle size distribution, the pyrite content, and the median pyrite grain size, liberated pyrite surface areas in the samples typically ranged from about 0.02 to 0.2 m^2 (Table 1). Coatings of 6 to 7 μm thickness were reported on three of the samples. The primary chemical constituents of the coatings were FeO (74-80 wt. %), SiO₂ (9-16 wt. %), CaO (3-5 wt. %), and SO₃ (0-14 wt. %).

Table 1 Paste pH and chemistry, mineral content, and pyrite characteristics related to oxidation.										
ID	GHN-JRM	ROC-NWD	SPR-JWM	PIT-VTM	GHN-KMD	PIT-RDL	GHN-JRM	GHN-JRM	BCS-VWL	GHN-KMD
	0009	0002	0002	0600	0096	0007	0001	0002	0004	0088
PASTE PH¹										
	3.97	4.4	6.26	7.16	2.56	2.29	2.14	2.15	4.29	2.63
WHOLE ROCK CHEMISTRY, WEIGHT PERCENT										
S	1.31	2.49	1.79	0.92	0.06	0.81	1.80	0.00	0.03	0.69
SO ₄	0.51	0.11	0.54	0.04	0.37	0.22	0.55	0.33	0.42	0.23
C	0.07	0.03	0.06	0.25	0.02	0.04	0.06	0.04	1.58	0.05
SULFUR-BEARING AND CARBONATE MINERAL CONTENT, WEIGHT PERCENT										
jarosite	1.7	0.01	NR	NR	1.4	1	2	0.01	2	NR
jarosite observed ²	Yes	No	No	No	Yes	Yes	Yes	Yes	Yes	No
gypsum	0.8	0.5	2	0.2	0.5	0.02	0.8	1.5	0.4	1
gypsum observed ²	No	No	No	No	No	No	Yes	No	Yes	No
calcite	0.5	0.1	0.5	2	0.2	0.2	0.4	0.3	0.2	0.3
calcite observed ²	Yes	No	Yes	Yes	No	No	No	No	No	No
PYRITE CHARACTERIZATION										
pyrite, wt. %	2	4	0.7 ³	2	0.1	1	3	0.01	0.1	1
coating, μm	0	0	7	6	0	0	0	7	0 ⁴	0
med. d ⁵ , μm	850	1100	100	250	12	45	154	190 ⁶	46	35
grains	662	393	1033	559	89	593	518	654	98	647

examined ⁷										
A _T (py) ⁸ , m ²	0.25	0.29	0.41	0.52	0.49	1.27	0.98	0.0032	0.13	1.66
A _L (py) ⁹ , m ²	0.20	0.20	0.053	0.20	0.018	0.11	0.38	0.0011	0.021	0.14

¹ McLemore et al. 2008

² Observed by New Mexico Tech or Mineral Services

³ Reported as 3 wt. % by New Mexico Tech. Alternative value selected is in closer agreement with pyrite

content based on post-leach sulfide content (0.5 wt. %), initial normative CIPW value reported by New

Mexico Tech (0.8 %), and Mineral Services Rietveld analysis (0.7 wt. %).

⁴ McSwiggen found no pyrite grains in the 60 mesh fraction of the sample but reported coating remnants.

⁵ Median sulfide grain diameter.

⁶ Number of grains reported is inconsistent with low pyrite content.

⁷ Pyrite grains examined to determine median diameter.

⁸ Total pyrite surface area.

⁹ Liberated pyrite surface area.

Humidity Cell Tests

As mentioned earlier, humidity cell testing was conducted at room temperature using compressed air, dried to zero humidity. This resulted in some cells being completely dried during the dry-air cycle. However, this did not happen consistently. Sometimes the residual water saturation would go to zero while for other weeks it would remain high. This can probably be attributed to preferential gas flow paths developing over time in the cells or a decrease in the air flow rate caused by uneven pressure distribution. Thus it is difficult to say how much moisture was present over the seven-day period for pyrite oxidation for each cell over time.

Initial pH values from five of the samples were in the range of 2.3-2.9, three ranged from 3.1-4, and the remaining two were 6.5 and 6.8. These values reasonably reflected those determined by McLemore et al. (2008) for paste pH (Figure 1). The pH reflected three trends: a neutral/basic group (pH 6.5-8.0), composed of SPR-JWM-002 and PIT-VTM-0600, a pH 5-6 group (BCS-VML-004), and an acidic group (pH 2.5-4.5) (Figure 2). The reproducibility of duplicated samples, SPR-JWM-002, GHN-KMD-0088 and GHN-JRM-0001 is demonstrated in Figure 2. Most cations and anions showed relatively high concentrations in the first few weeks of the humidity cell test, which is attributed to the initial pore water quality, the reaction of very small fines and soluble salts. Total iron concentrations generally corresponded with pH, with the lowest pH cells having the highest

iron concentrations and cells producing neutral or basic pH yielding iron concentrations at or below detection limits.

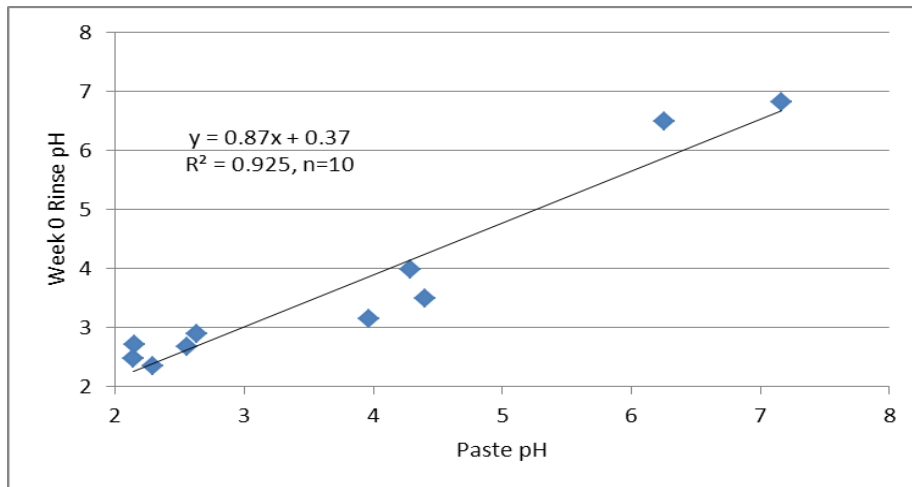


Figure 1 Effluent pH at week 0 correlated closely with paste pH.

Sulfate concentrations decreased rapidly in the initial stages of the experiment, reflecting removal of residual oxidation products generated during sample storage and preparation, as well as oxidation of highly reactive particles. In particular, such reaction could include oxidation of fine particles with high specific surface areas. Sulfate release ultimately plateaued toward the end of the period of record for most samples (Figure 2). Drainage quality for most samples was fairly stable after week 37, although release from some continued to oscillate within a constant range or decline slowly.

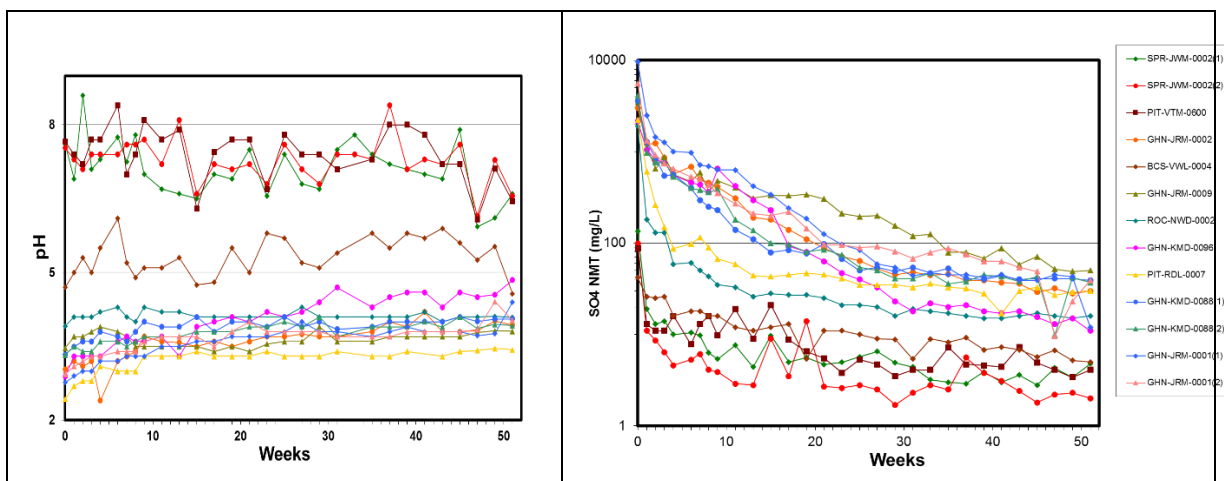


Figure 2 pH and sulfate concentration over time for all 10 samples. SPR-JWM-0002, GHN-KMD-0088 and GHN-JRM-0001 were run in duplicate.

Average sulfate release rates for weeks six through nine were calculated as an indicator of the rate of sulfate release after the initial rapid release, and the interval from week 37 to 52 was selected to represent a period of “fairly stable” sulfate release (Table 2). Ratios of the latter rate to that observed during weeks 6-9 was calculated to describe the degree to which sulfate release rates declined over the period of record. The ratios fell into two general ranges: 0.04-0.1 and 0.3-0.5 (Table 2). The lower range was associated with samples collected from trenches at the Goat Hill North rock pile. These samples were finer-grained materials that had been subjected to oxidation in the field for 30 to 35 years (McLemore et al., 2009). The remaining samples were generated from crushing larger rocks. The finer-grained Goat Hill North samples likely contained more labile sulfate generated from weathering in the field than the rock samples. The relatively rapid release of this sulfate resulted in a larger decline in sulfate release rates for the weathered samples. The trench samples also generally produced large changes in pH over this period, suggesting that the sulfate source was an acidic mineral rather than, for example, gypsum. Solid-phase analyses do not provide convincing corroboration for this suggestion (Table 1). Samples generating neutral or basic pH tended to produce low sulfate concentrations, whereas more acidic leachates generally had elevated sulfate concentrations. However, GHN-JRM-0009 consistently produced much higher sulfate concentration than the PIT-RDL-0007 despite a consistently higher pH.

Bacteriological results showed that sulfate-reducing bacteria and heterotrophic bacteria grew over time in all cells, even the ones not inoculated, however the *Acidithiobacillus* and *Leptospirillum sp.* were only detected in low numbers in a few of the cells (Richins et al. 2008). This may be due to lack of nutrients or the loss of microbes by pure water washes. Thus, it appears that *Acidithiobacillus* did not play a significant role in these humidity cells and pyrite was primarily oxidized abiotically by oxygen.

Pyrite oxidation rates were calculated for all ten samples based on the average weekly rates of sulfate release between weeks 37 and 52 and the calculated liberated pyrite surface area. Rates determined for two of the three samples in which pyrite content was reported as 0.1 percent or less were considerably higher than those for the remaining samples. The pyrite content of the latter seven samples ranged from 0.7 to 4 wt. %, and the following discussion focuses on the pyrite oxidation rates determined for these samples.

Table 2 Humidity cell data summary. Shaded values of dpy/dt indicate py ≤ 0.1 wt %.										
Sample ID	GHN-JRM 0009	ROC-NWD 0002	SPR-JWM 0002	PIT-VTM 0600	GHN-KMD 0096	PIT-RDL 0007	GHN-JRM 0001	GHN-JRM 0002	BCS-VWL 0004	GHN-KMD 0088
pH _o ¹	3.15	3.49	6.49	6.81	2.67	2.35	2.47	2.71	3.99	2.89

pH _i ²	3.11	3.52	6.88	6.95	3.12	2.80	2.96	3.19	4.26	3.25
pH _f ³	3.45	3.68	6.75	7.36	3.93	3.16	3.54	3.72	4.60	3.70
pH _f - pH _i	0.34	0.16	-0.13	0.41	0.81	0.36	0.58	0.53	0.34	0.45
dSO ₄ /dt ₀ ⁴	258	124	8.13	5.25	148	153	460	155	2.63	269
dSO ₄ /dt _i ⁵	36.2	3.10	0.50	0.896	28.0	6.39	32.4	31.8	1.23	25.0
dSO ₄ /dt _f ⁶	3.65	1.17	0.253	0.324	1.03	1.93	2.74	2.08	0.434	2.80
rate _f /rate _i ⁷	0.10	0.38	0.51	0.36	0.037	0.30	0.085	0.065	0.35	0.11
dpy/dt ⁸	9.3	2.9	2.4	0.80	29	8.8	3.6	950	10	9.8

¹ Initial rinse pH, arithmetic mean used for duplicate cells.

² Arithmetic mean pH, weeks 6-9.

³ Arithmetic mean pH, weeks 37-52.

⁴ Sulfate release rate, week 0, mol s⁻¹ × 10⁻¹⁰; assumes one week reaction time.

⁵ Average sulfate release rate, weeks 6-9, mol s⁻¹ × 10⁻¹⁰.

⁶ Average sulfate release rate, weeks 37-52, mol s⁻¹ × 10⁻¹⁰.

⁷ Ratio of average sulfate release rate for weeks 37-52 to that for weeks 6-9.

⁸ Average pyrite oxidation rate, weeks 37-52, mol m⁻² s⁻¹ × 10⁻¹⁰.

The resultant oxidation rates ranged from 0.8 × 10⁻¹⁰ to 9.8 × 10⁻¹⁰ mol m⁻² s⁻¹, with all but one value exceeding 2 × 10⁻¹⁰ mol m⁻² s⁻¹ (Table 2). The calculated rates exhibited a mild dependence on pH although this dependence must be viewed with caution. The data fall into two clusters at roughly pH 3.5 and 7.3 (Figure 3). The intent of this analysis was to aid in description of the data and not to deduce a mechanistic interpretation. It should further be noted that the two points near pH 7.3 were both generated by samples in which pyrite coatings of 6-7 μm were detected. These coating likely contributed to the lower oxidation rates observed for these samples.

The pyrite oxidation rates observed were lower than those reported for oxidation of pyrite present in greenstone samples (Lapakko and Antonson 2006) (Figure 3). Using the two linear regressions as descriptors, the Questa oxidation rates are about 30 to 60 percent of those for the greenstone samples. One factor contributing to this discrepancy is the difference in reaction conditions between the two experiments. In the greenstone experiments, no air was introduced to the humidity cells, and typically 130 to 150 mL of water was retained in the cells throughout the weekly cycle. Pyrite

oxidation in this experiment was described as occurring in the fine fraction of rock particles that were in contact with oxygen saturated water. This was consistent with the agreement of observed rates with those reported by Williamson and Rimstidt (1994).

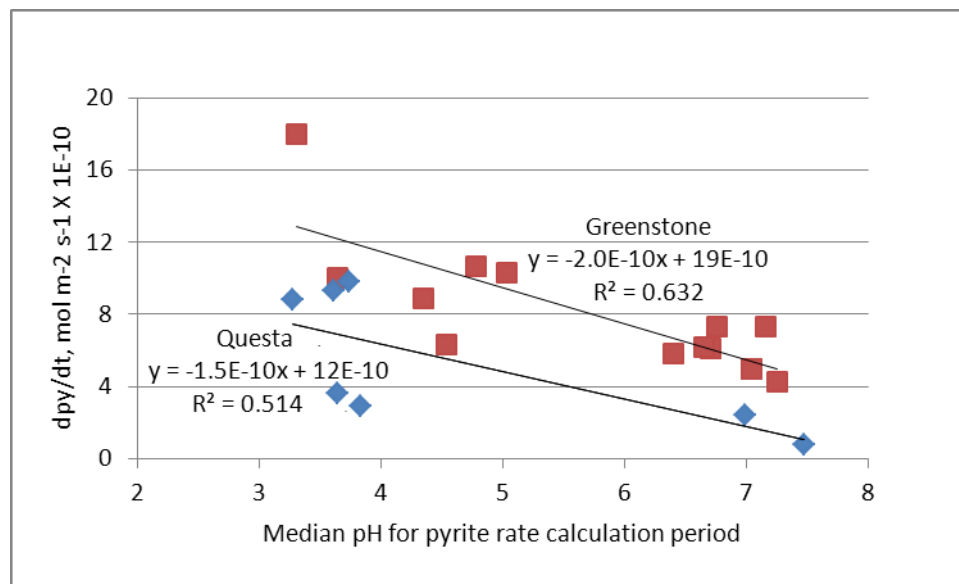


Figure 3 Pyrite oxidation rates for the Questa samples were lower than those reported for greenstone samples (Lapakko and Antonson 2006). The drier oxidation conditions of Questa samples during the weekly cycle likely contributed to the lower rates.

In contrast, the cells in the present study were subjected to three days of dry air following the day during which samples drained. During this day, oxidation likely occurred in the presence of oxygen saturated water. During the next three days water evaporated from the cell, sometimes to total dryness. Thus, during this period, oxidation could occur with pyrite grains in contact with oxygen saturated water, water saturated air as observed by Jerz and Rimstidt (2004), or with air of variable water saturation. Because it is not possible to confidently describe the precise reaction conditions, oxidation rates for several possible conditions were calculated to compare theoretical rates (i.e. Williamson and Rimstidt 1994 and Jerz and Rimstidt 2004) with those observed. The overall range of rates calculated for various time periods for abiotic oxidation by oxygen in water and oxidation in humid air was 0.3×10^{-10} to 7.2×10^{-10} mol m⁻² s⁻¹. The observed range for the samples in this study was 0.8×10^{-10} to 9.8×10^{-10} mol m⁻² s⁻¹, within or slightly above the theoretical range.

SUMMARY

Rates of pyrite oxidation were determined for seven waste rock samples subjected to humidity cell testing for one year based on observed rates of sulfate release and liberated pyrite surface area.

Liberated pyrite surface area was determined using pyrite content and size distributions of pyrite grains and the rock subjected to testing. The equation used for this determination yielded rates that were consistent with those reported in the literature for samples with pyrite contents between 0.7 and 4 percent. For two samples with pyrite contents near 0.1 percent, the calculated rates were one and three times those for the samples of higher pyrite content. The oxidation rate for a sample with a reported pyrite content of 0.01 percent was almost three orders of magnitude above the range for higher pyrite contents. This suggests that the method yields reasonable results for sample with pyrite contents above 0.1 percent, but for samples with lower pyrite content the method has limitations. For samples of low pyrite content the method may underestimate the liberated pyrite surface area due to low pyrite concentrations or the occurrence of pyrite as very fine grains on rock surfaces. Alternatively, a highly reactive sulfide or sulfate mineral may have been present at low concentrations in these samples.

ACKNOWLEDGEMENTS

Chevron Mining provided funding for the humidity cell testing. Kelly Donahue of Brown and Caldwell provided initial review of sample collection methods and general petrology. Mike Moncur of Alberta Innovates – Technology Futures and Bob Seal of the United States Geological Survey provided constructive review of the draft submitted.

REFERENCES

- ASTM International (2013) D5744-13e, Standard test method for laboratory weathering of solid materials using a humidity cell. In Annual book of ASTM Standards, 11.04. American Society for Testing and Materials International, West Conshohocken, PA. 23 p. (<http://www.astm.org/Standards/D5744.htm?A>).
- Chevron (2005) Standard operating procedure no. 5: Sampling outcrops, rock piles, and drill core (solid), rev. 5v8, 2/07/05: unpublished report to Chevron. 19 p.
- Dunbar, N., Heizler, L. and Sweeney, D. (2008) DRA-4. Mineralogical characterization of Questa rock-pile samples by petrographic and electron microprobe analysis: unpublished report to Molycorp, Inc., DRA-4. 19 p.
- Jerz, J.K. & Rimstidt, D.J. (2004) Pyrite oxidation in moist air. *Geochim. Cosmochim. Acta* 68. p. 701-714.
- Lapakko, K.A. and Antonson, D.A. (2006) Pyrite oxidation rates from humidity cell testing of greenstone rock. In Proc. 2006, 7th ICARD, March 26-30, 2006, St. Louis MO. Published by ASMR, 3134 Montavesta Rd., Lexington, KY 40502. p. 1007-1025.
- McLemore, V.T., Heizler, L., Dunbar, N., Phillips, E., Donahue, K., Sweeney, D., Dickens, A. and Ennin, F. (2008) Petrographic Analysis of Humidity Cell Samples: unpublished report to Chevron, Task B1.5.2. 29 p. plus appendices.
- McLemore, V.T., Walsh, P., Donahue, K., Gutierrez, L., Tachie-Menson, S., Shannon, H.R. and Wilson, G.W. (2005) Preliminary status report on Molycorp Goathill North trenches, Questa, New Mexico, 2005 National Meeting, of the American Society of Mining and Reclamation. American Society of Mining and Reclamation, Breckenridge p. 507-532.

- McLemore, V.T., Heizler, L., Donahue, K. and Dunbar, N. (2009) Characterization of weathering of mine rock piles: Example from the Quest mine, New Mexico, USA. In Proc. Securing the Future and 8th ICARD, June 23-26, 2009, Skellefteå, Sweden, CD-ROM. 10 p.
- McSwiggen, P. (2008a) Sulfide mineral liberation. Technical memo by Peter McSwiggen, McSwiggen & Associates, P.A. Micro Analytical Services, St. Anthony, MN. 29 July 2008. 11p.
- McSwiggen, P. (2008b) Part B3-Sulfide mineral coatings in unleached samples. Technical memo by Peter McSwiggen, McSwiggen & Associates, P.A. Micro Analytical Services, St. Anthony, MN. 28 August 2008. 3 p.
- Mineral Services (2008) Petrographic and mineralogical characterization of 14 samples from the rock piles of the Questa molybdenum mine (New Mexico, USA). Report prepared for Mark J. Logsdon, Geochimica Inc. by Mineral Services Canada Inc., North Vancouver, B.C. 16 April 2008. 80 p.
- Richins, B., Eschler, J., Kennedy, J. and Adams, D.J. (2008) Questa Mine Site: Humidity Cell Microbial Evaluation. University of Utah.
- Williamson, M.A. and Rimstidt, J.D. (1994) The kinetics and electrochemical rate-determining step of aqueous pyrite oxidation. *Geochim. Cosmochim. Acta*, 58. p. 5443-5454.